UDK 536.248.2:532.529.5

Doroshenko A.[1], Guangming Chen[2], Shestopalov K.[1,2], Khlieva O.[1]

[1] Odessa National Academy of Food Technologies. Odessa,
[2] Ningbo Institute of Technology, Zhejiang University, China
khliyev@ukr.net

Heat and mass transfer at cooling of gases and liquids in ceramic evaporative cooler. Part I

In this part of paper, a method for the determination of the efficiency and limitations of the evaporative cooling process is presented. Ceramic is employed as a packing material in the evaporative equipment. It is shown that the experimental efficiency of the ceramic packing is 10-20% higher as compared to packings made from aluminum foil and multichannel polycarbonate plates because of the absence of traditional liquid film on the packing surface, and due to the absolute wettability of the ceramic packing.

1. Introduction. Evaporative cooling is efficient for dry and hot climate conditions (when the humidity ratio of the ambient air x_a<12…14 g kg^{-1}). The development of the indirect evaporative coolers is of particular interest because the air flow is cooled without contact with water, meaning that the humidity ratio of the handled air is unchanged. The application of a heat-driven absorption cycle, which consists of the preliminary dehumidification of the air followed by its further use for evaporative cooling, is the basis for the creation of alternative solar refrigeration and air conditioning systems (RACS).

The wide practical application of desiccant-evaporative cooling methods in modern solar cooling and heating systems requires solutions to the following problems: selection of working fluids (desiccants) that provide high absorption capacity and show minimum adverse effect on structural materials; creation of effective heating circuits for desiccant regeneration, which is essential to the development of high quality solar collectors, which can provide the required temperature level for regeneration; the decrease of the energy inputs for transport of the working fluids (flows of air, water, and desiccant). The development of desiccant-evaporative systems can remove climatic limitations for the application of evaporative methods of cooling and significantly enhance energy and ecology characteristics of alternative RACSs.

The number of studies dedicated to investigating the capabilities of the open absorption cycle with regard to cooling and air conditioning continuously increases because such systems are easy to design, feature simple operation, and enjoy high reliability and durability [1, 2].

One of the most important considerations for such systems is the process of coupled heat and mass transfer in the packing of the appropriate device: absorber, desorber (for the systems with desiccant regeneration in desorber), direct evaporative cooler (DEC), indirect evaporative cooler (IEC), and cooling tower (CTW). As stated in paper [3], the packing can vary in structure (structured and random) and material

(metal, plastic, paper, cotton, ceramics, etc.). The problem of film distribution on the packing surface (the problem of maximum wettability) is of great importance because the dry part of the packing is eliminated from the heat and mass exchange process, resulting in a decreasing in device efficiency. Nozzles and other devices can be used to ensure uniform distribution of liquid and total wetting of the packing.

To avoid these problems, porous materials (ceramics) were proposed as materials for packing elements for evaporative cooling. Recently, much theoretical and experimental research has been performed to study the application of porous materials for cooling purposes [3-9].

The main objective of this research is the development of constituent devices, based on ceramic modules, for innovative, high-performance solar-driven desiccant-evaporative systems with direct desiccant regeneration in the solar collector-regenerator. Such systems are intended for commercial application in different domestic and industrial cooling, refrigeration, and air conditioning systems.

2. Efficiency and natural limitations of evaporative cooling. Traditionally, the wet bulb air temperature at the entrance of the evaporative device t_{wb}^1 is considered as a natural limit for water cooling. At the exit from the device, the saturation condition of the air with the temperature of entering water for cooling t_w^1 (the air at the exit with enthalpy h_a^{2*}) is considered as a limitation. The efficiency of the water cooling in the CTW can be characterized by the value of E_w, which is determined from the ratio of the actual rejected heat from water to the ideal one when the water temperature at the exit of the evaporative device $t_w^2 = t_{wb}^1$:

$$E_w = \frac{t_w^1 - t_w^2}{t_w^1 - t_{wb}^1}. \quad (1)$$

It is obvious that $E_w = \Delta/\Delta_{id}$, where $\Delta = t_w^1 - t_w^2$, is the range of the cooling. The terms "the degree of water cooling" or "water cooling efficiency" were used for the value of E_w [10]. The value of E_w characterizes only one part of the process in the device. The efficiency of the air condition changes can be determined by the value of E_a, which is the ratio of the heat carried out from the device by the air to the maximum heat determined from $h_a^2 = h_a^{2*}$:

$$E_a = \frac{h_a^2 - h_a^1}{h_a^{2*} - h_a^1}, \quad (2)$$

where h_a^1, h_a^2 – air enthalpy at the entrance and at the exit of the evaporative device.

By analogy with E_w, the value of E_a is named "the efficiency of the air" in the device. It is obvious that at given E_w, the higher the air efficiency, the lower the energy consumption of the ventilator of the cooler, and the lower the specific energy input.

The following assumptions are made:

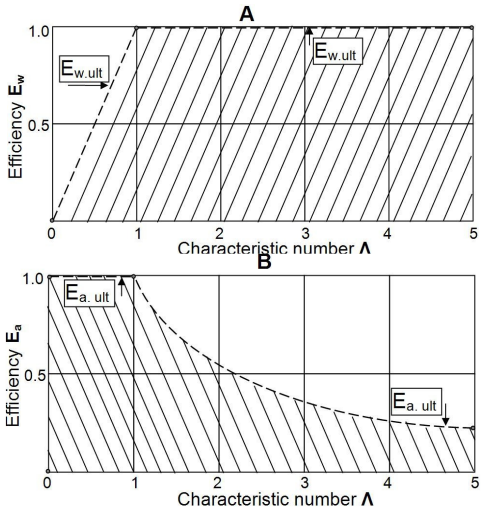

Fig. 1. *Ultimate value of water cooling degree (A) and air efficiency (B) in an evaporative cooler.*

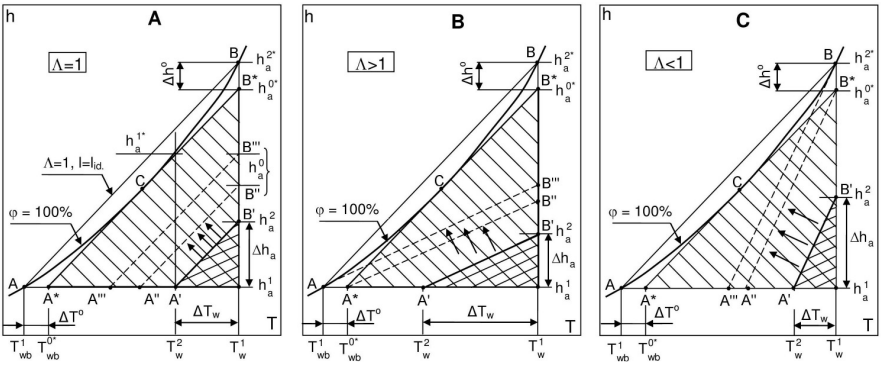

Fig. 2. *Limitations of evaporative cooling of water and the degree of air efficiency*

$$E_w = f\left(l = \frac{G_a}{G_w}, t_w^1, t_{wb}^1\right), \tag{3}$$

$$E_a = f\left(l = \frac{G_a}{G_w}, t_w^1, t_{wb}^1\right). \tag{4}$$

where l – relative flow rate; G_a, G_w – air and water mass flow rate, kg s^{-1}.

Service conditions of the evaporative cooler are characterized by the characteristic number Λ [1]:

$$\Lambda = \frac{l}{l_{id}}. \tag{5}$$

Additional explanation of the parameter Λ is given below.

The variations for E_w and E_a are shown in Fig. 1 for the ultimate values of theoretical curves that can be considered for any type of the packing [10]. The dashed sector represents the possible values of the process efficiencies. It can be seen that the increase of the relative air flow l results in the increase of E_w and decrease of E_a. The lower values of air efficiency correspond to the higher values of the water cooling degree. E_w and E_a are independent from the mode of the l behavior (by the variation of air flow or water flow).

The real limiting values of the water cooling and air heating, besides the values of t_{wb}^1 and t_w^2, are determined by the ratio of $l = G_a / G_w$. The working process line is A^*B^* in Fig. 2. In any cross-section of the device, the temperature of water is higher than the air wet bulb temperature. The state when these temperatures are equal is located on the saturation line. The position when the working line touches the saturation line is its ultimate value. In this point of tangency, the difference $h_a^* - h_a$ becomes zero. The typical positions of the working line in the field of the wet air diagram are discussed below.

In Fig. 2B the case is shown when the l is high. The increase of exchange surface results in parallel movement of the working line A^*B^* to the saturation line. The location AB‴ (area F = ∞) is ultimate (in the lower section of the device the factor vanishes). The water can be cooled until t_{wb}^1 ($t_{wb}^1 = t_{wb}^2$), and in the lower section of the device the conditions of the equilibrium are performed. The limit of the air heating, which is determined by h_a^0, is lower than the value of h_a^{2*} (point B*), it is determined by the temperature of the water entering the evaporative cooler:

$$E_w^0 = \frac{t_w^1 - t_w^2}{t_w^1 - t_{wb}^1} = E_w, \tag{6}$$

$$E_a^0 = \frac{h_a^2 - h_a^1}{h_a^0 - h_a^1} > E_a. \tag{7}$$

When the l is low (Fig. 2C), the tangency point of the ultimate position of the working line and the saturation line is located in the upper section of the device. The water can be cooled up to the temperature determined by the ultimate line A‴B ($t_{wb}^0 > t_{wb}^1$), and in the upper section the conditions of the equilibrium are fulfilled:

$$E_w^0 = \frac{t_w^1 - t_w^2}{t_w^1 - t_{wb}^{0*}} > E_w, \tag{8}$$

$$E_a^0 = \frac{h_a^2 - h_a^1}{h_a^{2*} - h_a^1} = E_a. \tag{9}$$

In Fig. 2A the case is shown in which the tangency point C of the working line ultimate position with the saturation line (F = ∞) is located between points A and B. Here at both ends of the device, the conditions are different from equilibrium:

$$E_w^0 = \frac{t_w^1 - t_w^2}{t_w^1 - t_{wb}^{0*}} > E_w, \tag{10}$$

$$E_a^0 = \frac{h_a^2 - h_a^1}{h_a^{0*} - h_a^1} > E_a, \tag{11}$$

$$E_w^0 = E_a^0. \tag{12}$$

Depending on the value of l, the equilibrium state can take place at either the topping or bottoming end of the cooler. The equilibrium state at both ends cannot occur simultaneously – this can be explained by the curvature of the saturation line. In general cases, the new values of the limitation for the evaporating process of cooling are determined from Equations (13) and (14):

$$t_{wb}^0 = f\left(t_w^1, t_{wb}^1, l = \frac{G_a}{G_w}\right), \tag{13}$$

$$h_a^0 = f\left(t_w^1, t_{wb}^1, l = \frac{G_a}{G_w}\right). \tag{14}$$

Thermodynamic equilibrium at the entrance and exit of the CTW corresponds to the "ideal" model of the counter flow device (F = ∞). The essence of the model is determined as follows: the optimal process in CTW is the process in which the departing cooled water and the fresh air entering the CTW, as well as the exhaust air and entering warm water, reach thermodynamic equilibrium at the steady-state heat and mass transfer process. The boundary conditions for the bottom of the device are $t_w^2 = t_{wb}^1$; for the top $t_a^2 = t_w^1$; relative humidity $\varphi_a^2 = 100\%$ ($h_a^2 = h_a^{2*}$, point B in Fig. 2).

For the adiabatic process for counter flow conditions (recirculation of water through the cooler without outside heat load), the equations of heat balance are:

$$G_a h_a^1 + G_w^1 c_w t_w^1 = G_a h_a^2 + G_w^2 c_w t_w^2, \tag{15}$$

$$G_a h_a^1 + G_w^1 h_w^1 = G_a h_a^2 + G_w^2 h_w^2. \tag{16}$$

where c_w – constant pressure specific heat, kJ kg^{-1} K^{-1}; G_w^1, G_w^2 – water mass flow rate at the entrance and at the exit of the evaporative device, kg s^{-1}; h_w^1, h_w^2 – water enthalpy at the entrance and at the exit of the evaporative device.

The equation of mass balance is:

$$G_a(x_a^2 - x_a^1) = G_w^1 - G_w^2, \tag{17}$$

where x_a^1, x_a^2 – moisture content of air at the entrance and at the exit of the evaporative device, g kg^{-1}.

Thus:

$$l^1 = \frac{G_a}{G_w^1} = \frac{c_w\left(t_w^1 - t_w^2\right)}{\left(h_a^2 - h_a^1\right) - c_w t_w^2\left(x_a^2 - x_a^1\right)}, \tag{18}$$

$$l^1 = \frac{G_a}{G_w^1} = \frac{h_w^1 - h_w^2}{\left(h_a^2 - h_a^1\right) - h_w^2\left(x_a^2 - x_a^1\right)}, \tag{19}$$

where $l^1 = \frac{G_a}{G_w^1}$ is a relative air flow. For such a model:

$$l_{id} = \left(\frac{G_a}{G_w^1}\right)_{id} = \frac{c_w(t_w^1 - t_{wb}^2)}{\left(h_a^{2*} - h_a^1\right) - c_w t_{wb}^2\left(x_a^{0*} - x_a^1\right)}, \tag{20}$$

where l_{id} is a relative minimal air flow. When $l = l_{id}$ and $F = \infty$, both ends of the CTW achieve equilibrium condition. From Equation (20), it follows that $l_{id} = f(t_w^1, t_a^1, x_a^1)$; thus the value of l_{id} is determined by three independent parameters.

The limiting value of E_w, which corresponds to the condition F = ∞, can be found from:

$$l^2 = \frac{G_a}{G_w^2} = \frac{c_w(t_w^1 - t_w^2)}{\left(h_a^2 - h_a^1\right) - c_w t_w^1\left(x_a^2 - x_a^1\right)}, \tag{21}$$

$$l_{id}^2 = \left(\frac{G_a}{G_w^2}\right)_{id} = \frac{c_w(t_w^1 - t_w^2)}{\left(h_a^{2*} - h_a^1\right) - c_w t_w^1\left(x_a^{0*} - x_a^1\right)}, \tag{22}$$

$$E_w = \frac{t_w^1 - t_w^2}{t_w^1 - t_{wb}^1} = \frac{(h_a^2 - h_a^1) - c_w t_w^1(x_a^2 - x_a^1)}{\left(h_a^{2*} - h_a^1\right) - c_w t_w^1\left(x_a^{0*} - x_a^1\right)}, \tag{23}$$

$E_{w\,lim} \cong \Lambda$, when $\Lambda \le 1$ and $E_{w\,lim} = 1$, when $\Lambda \ge 1$.

Description of the process in the CTW by the degree of cooling is not enough. It can be supposed the existence of the relation $E_a = f(\Lambda)$. Thus:

$$\Delta t_w = t_w^1 - t_w^2 = \left(h_a^1 - h_a^2\right) l = \left(h_a^{1*} - h_a^{2*}\right) l_{id}, \tag{24}$$

$$\frac{h_a^{1*} - h_a^{2*}}{h_a^2 - h_a^1} \cong \Lambda, \tag{25}$$

$$\frac{E_w}{E_a} = \frac{h_a^{1*} - h_a^{2*}}{h_a^{1*} - h_a^1} \frac{h_a^{1*} - h_a^1}{h_a^2 - h_a^1} = \frac{h_a^{1*} - h_a^{2*}}{h_a^2 - h_a^1}, \tag{26}$$

$$\frac{E_w}{E_a} \cong \Lambda. \tag{27}$$

Equation (27) is approximative. The received relation allows the determination of the limiting values of water cooling degree and the efficiency of air in the cooler:

$$E_{a\,\lim} = \lim_{F \to \infty} E_a = 1.0, \text{ when } \Lambda \le 1.0;$$

$$E_{w\lim} = \lim_{F\to\infty} E_w \cong \Lambda, \text{ when } \Lambda \le 1.0;$$

$$E_{a\lim} = \lim_{F\to\infty} E_a \cong \frac{1}{\Lambda}, \text{ when } \Lambda \ge 1.0;$$

$$E_{w\lim} = \lim_{F\to\infty} E_w = 1, \text{ when } \Lambda \ge 1.0.$$

In the research study of Doroshenko [10], the empirical formulas useful for practical application are suggested for the determination of the process efficiency values in CTW:

$$E_w = c\,(1 - e^{-1.1\,\Lambda}), \tag{28}$$

$$E_a = c\,(1 - e^{-1.1\,\Lambda})\,\Lambda^{-1}. \tag{29}$$

where c is determined experimentally depending on the material of the packing.

3. Experimental study of the heat and mass transfer processes in evaporative coolers. A test rig was built for experimental investigations of the evaporative coolers' working characteristics. A schematic diagram and photograph of the test rig are shown in Fig 3. The test rig provides the opportunity of studying the working processes in CTW and DEC, as well as in IEC. The ambient air after heat and humidity handling (heating in the air heater 1 and moistening through the bypass line 7 by the air flow leaving the evaporative cooler) through ventilator 2 enters the working chamber 3, where the evaporative cooler module is installed. The variable speed motor of the ventilator allows for regulation of the air flow rate in the device. The temperature of the air is regulated in the channel electric heating coil 1, where it can reach 70 °C. The main part of the test rig, where the evaporative cooler module is located, is made with an inspection window (detachable cap) fabricated from thick-walled transparent plexiglass. Dimensions of the chamber are 460×400×180mm; throughput performance of the full air flow is up to 3500 $m^3\,h^{-1}$. Air flow meter 6 and air flow regulators 8 and 9 are installed in the air line.

Circulation of the water through the evaporative cooler module is organized by water pump 13 with regulated flow rate. The water flow rate is measured by RS-type flow meter 10. The water through the discharge line enters distribution chamber 4, from which it comes for packing sprinkling. The constructive embodiment of all HMTE is unified (CTW, DEC, IEC). They all are constructed as cross-flow devices in which vertical multichannel plates from ceramic porous material (CPM) are utilized as a main element of the packing. Water chamber 11 consists of five pockets. This provides differential measurement of water flow rate and the latching of its lengthwise surging by air flow. All of the pipelines are thermally isolated. Temperature and relative humidity of the air are measured before and after the working chamber (mercurial thermometers and RTD sensors 17 and 18). K-type thermocouples are used for temperature measurement around the cycle, along with a multichannel measuring converter.

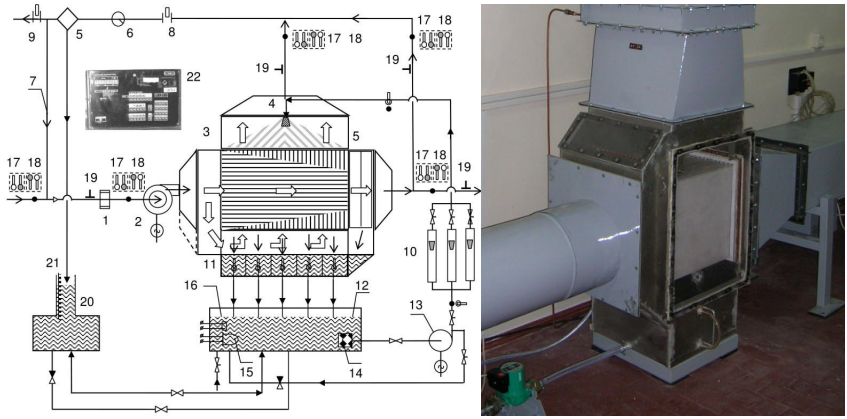

Fig. 3. *Schematic diagram and photograph of the test rig for the investigation of the cross-flow heat and mass transfer devices for direct and indirect evaporative cooling of water and air. 1 – electric heater; 2 – ventilator; 3 – working chamber; 4 – liquid distributor; 5 – spray separator; 6 – air flow meter; 7 – recirculating line; 8, 9 – air flow regulator; 10 – water flow meters; 11 – sectional measurer of the liquid flow rate; 12 – water tank; 13 – water pump; 14 – filter; 15 – water heater; 16 – water temperature regulator; 17, 18 – mercury thermometer and RTD sensor; 19 – pressure gauge; 20 – tank for the measurement of liquid retention; 21 – scale bar; 22 – control box.*

The test rig provides the experimental investigations of designed evaporative coolers with the packing made from equidistantly located CPM plates with ribbing, which create multichannel regular packing. Previously, the experimental research of evaporative cooling in lengthways-corrugated elements made from aluminum foil paper and multichannel polymeric structures was conducted at the Odessa State Academy of Refrigeration [10, 11]. The value of the equivalent diameter of the channels was varied in the range of 15…20mm; the constructive surface of the packing in a volume unit was varied in the range of 170…200 $m^2 m^{-3}$. Obtained recommendations along with the results of the studies of Doroshenko [10, 11], were used in the manufacturing of the evaporative cooler modules made from CPM. The working range of air velocity in the channels of the packing was varied in the range of 1.0…7.0 m s^{-1}. The value of the ratio of air and water was $l = G_a / G_w \approx 1.0$ for the evaporative coolers of water, and the water sprinkling density was $q_w = 5…18$ $m^3 m^{-2} h^{-1}$.

Measurement accuracy of the main data is determined by the accuracy of the devices, and it was calculated for each experiment (for the heat balance the accuracy was about 12%).

The following findings were drawn from the experiment. The increase of water flow rate G_w from "dry" regime to the value of the water sprinkling density of $q_w = 10$ $m^3 m^{-2} h^{-1}$ did not result in an appreciable increase of pressure drop when air passes through the "wet" part of the IEC packing. This was explained by a practical absence of liquid film on the surface of the packing. The traditional phenomenon of flooding (evacuation of liquid from the packing of the device by air flow and the decreasing of

the device capacity up to zero) for the cross-flow scheme is fully absent up to the value of v_a < 8-10 m s^{-1}; phenomenon of lengthways drifting of liquid, resulting in its unfavorable distribution in the volume of the packing and removal from the layer, is also fully absent – which can be explained by absence of liquid film on the surface of the packing as well. The transition to a cross-flow scheme provides the decrease of Δp, and consequently the decrease of rated power inputs compared to counter-flow mode, and also provides the possibility of further increase of the capacity. Besides, when several devices are located in one cooling unit, the cross-flow linear mode is an optimal solution for the arrangement of the devices.

The liquid retardation in the layer of the packing substantively provides high value of the heat and mass transfer surface, and thus it results in acceptable efficiency of the evaporative cooling process. The accumulation of the liquid in the volume of the ceramic packing takes place practically instantly and in such a way that the total surface for heat and mass transfer is formed. A circulating method was used in the study for the determination of the liquid retardation in the layer of the packing, based on the principle of conservation of the liquid while working in a closed circuit [1].

The liquid is pumped to the device from the calibrated tank (12-20) and it drains into it. The difference between the levels of the liquid before activation of the device and when the device is operated is proportional to the retention of the packing layer. During the operation, the level of the liquid was changed due to liquid evacuation and evaporation. Developed methodology allowed these ingredients to be taken into account to determine full liquid retardation.

For IEC during the experiment, the ratio of the primary and secondary air flows was $l_{IEC} = G_P/G_S = 1.0$. Thermal efficiency of the IEC for primary and secondary air flows is determined from:

$$E_p = \frac{t_p^1 - t_p^2}{t_p^1 - t^0}, E_s = \frac{t_s^1 - t_s^2}{t_s^1 - t^0}, \tag{30}$$

where t^0 is the air wet bulb temperature at the entrance of the device similar to DEC, but it is 1.5…2.0°C higher because of thermal conductivity of the dividing wall and inner heat flux from primary to secondary air flow.

On average, the value of E_p is in the range of 0.6…0.9, which is substantially higher than the values of the process efficiency for the film-type packing composed from multichannel polycarbonate plates E_p = 0.55-0.75 [1]. This is determined by the value of liquid retardation. According to Fig. 5A, the efficiency of the process E_p decreases as the moisture content of the ambient air increases. The efficiency of the primary air flow process improves when the temperature of the air at the entrance of the device is increased (Fig. 5B). Thermal efficiency of the IEC for secondary air flow is 10-15% higher on average as compared to the efficiency for the primary air flow. Consequently, the working range of the value of l_{IEC} can be increased.

The results of water cooling during the evaporative process in CTW are shown in Fig. 4, where the efficiency of the process (the water cooling degree) is the function of the characteristic number $\Lambda = l / l_{id}$, where $l = G_a / G_w$ (the value of l_{id} corresponds to the ideal design of the water cooler and is determined by t_w^1 and t_{wb}^1).

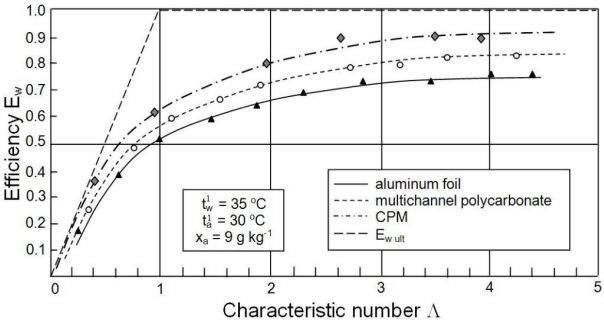

Fig. 4. *Efficiency of the water cooling process in CTW.*

The value of the flow ratio was $l \approx 1.0$; the density of sprinkling was $q_w = 5…18$ $m^3m^{-2}h^{-1}$. It can be seen from Fig. 4 that the efficiency of packing made from CPM is 10–20% higher compared to previously received experimental results for packing constructed of aluminum foil and multichannel polycarbonate plates. The results received in application to the process of evaporative cooling can be described by the Equations (28) – (29).

The following results will be presented in the second part of article:

- design and development of the evaporative equipment for solar desiccant cooling systems;
- the perspectives of solar liquid desiccant cooling systems, analysis of the results.

REFERENCES:

1. *Дорошенко А.В., Глауберман М.А.* Альтернативная энергетика. Солнечные системы теплохладоснабжения: монография. – Одесса: ОНУ, 2012. – 446 с
2. *Xie, G., Wu, Q., Fa, X., Zhang, L., Bans, P.* A novel lithium bromide absorption chiller with enhanced absorption pressure. // Applied Thermal Engineering. – 2012. – V. 38. – P.1-6.
3. *Zhao, X., Liu, S., Riffat, S.B*. Comparative study of heat and mass exchanging materials for indirect evaporative cooling systems. Building and Environment. – 2008. – V. 43. – P. 1902–1911.
4. *Gomes, E.V., Martinez, F.J., Diez, F.V., Leyva, M.J., Martin, R.H.*, 2005. Description and experimental results of a semi-indirect ceramic evaporative cooler. // Int. Journal of Refrigeration. –2005. – V.28. – P. 654-662.
5. *He, J., Hoyano, A*. Experimental study of cooling effects of a passive evaporative cooling wall constructed of porous ceramics with high water soaking-up ability // Building and Environment. – 2010. – V. – 45. – P. 461–472.
6. *Ibrahim, E., Shao, L., Riffat, S.B.* Performance of porous ceramic evaporators for building cooling application. // Energy and Buildings. – 2003. – V. 35. – P. 941–949.
7. *Martínez, F.J., Gómez, E.V., García, C.M., Requena, J.F., Gracia, L.M., Navarro, S.H, Guimaraes, A.C., Gil, J.M.* Life cycle assessment of a semi-indirect ceramic evapora-

tive cooler vs. a heat pump in two climate areas of // Spain. Applied Energy. – 2011. – V. 88. – P. 914-921.
8. *Pires, L., Silva, P.D., Gomes, J.P.* Performance of textile and building materials for a particular evaporative cooling purpose. // Experimental Thermal and Fluid Science. – 2011. – V. 35. – P. – 670–675.
9. *Riffat, S.B., Zhu, J.* Mathematical model of indirect evaporative cooler using porous ceramic and heat pipe. // Applied Thermal Engineering. –2004. – V. 24. – P. 457-470.
10. *Дорошенко А.В.* Компактная тепломассообменная аппаратура для холодильной техники (теория, расчет, инженерная практика). Дисс. … доктора технических наук. – Одесса, 1992. – 340 с.
11. *Дорошенко А.В., Горин А.* Солнечные холодильные и кондиционирующие системы // Отопление, водоснабжение, вентиляция + кондиционеры. – 2005. – №1. – С. 67–72.
12. *Лавренченко Г., Дорошенко А.* Разработка косвенно-испарительных воздухоохладителей для систем кондиционирования // Холодильная техника. – 1988. – №10. – С. 33 -38.

Дорошенко А.В., Chen Guangming, Шестопалов К.А., Хлиева О.Я.

Тепломассообмен при охлаждении газов и жидкостей в испарительных охладителях с керамической насадкой. Часть I

АННОТАЦИЯ

В первой части работы представлена методика оценки эффективности процессов испарительного охлаждения. Рассматривается возможность использования керамических материалов для изготовления насадки испарительных охладителей. В работе показано, что экспериментально оцененная эффективность при использовании керамической насадки на 10-20% выше, чем при использовании насадки из алюминиевой фольги или многоканальных поликарбонатных панелей, что объясняется отсутствием традиционной пленки жидкости на поверхности насадки и полной смоченностью керамической насадки.

Дорошенко О.В., Chen Guangming, Шестопалов К.О., Хлієва О.Я.

Тепломасообмін при охолоджуванні газів ті рідин в випарювальних охолоджувачах з керамічною насадкою. Частина I

АНОТАЦІЯ

У першій частині роботи представлена методика оцінки ефективності процесів випарювального охолодження. Розглядається можливість використання керамічних матеріалів для виготовлення насадки випарювальних охолоджувачів. У роботі показано, що експериментально оцінена ефективність при використанні керамічної насадки на 10-20% вища , ніж при використанні насадки з алюмінієвої фольги або багатоканальних полікарбонатних панелей , що пояснюється відсутністю традиційної плівки рідини на поверхні насадки і повним змоченням керамічної насадки.